All-Fiber Vector Bending Sensor Based on a Multicore Fiber With Asymmetric Air-Hole Structure

Dawid Budnicki [ID], Itxaso Parola, Łukasz Szostkiewicz, Krzysztof Markiewicz, Zbigniew Hołdyński [ID], Grzegorz Wojcik, Mariusz Makara, Krzysztof Poturaj, Małgorzata Kuklińska, Paweł Mergo [ID], Marek Napierała, and Tomasz Nasiłowski

Abstract—In this article we present an all-fiber vector bend sensor by means of a self-fabricated micro-structured multicore optical fiber. The reported solution is based on differential intensity variations of the light transmitted along the cores whose changes are influenced by the bending angle and orientation. The unique asymmetric structure of the air-holes in the optical fiber provides each core with different confinement losses of the fundamental mode depending on the bending radius and orientation, making each of the cores bend-sensitive in a range of at least 80°. It has been experimentally demonstrated that the reported sensor enables the bending angle and orientation to be detected in a full range of 360° without any dead-zones, and the possibility of end point detection with millimeter precision. Additionally, a reconstruction of the bending vector has been carried out theoretically, and a good match can be observed between the experimental and theoretical data.

Index Terms—Bend sensor, intensity sensor, microstructured optical fiber, multicore fiber, optical fiber sensor, vector sensor.

I. INTRODUCTION

BENDING deformation measurement plays an important role in the fields of structural health monitoring (SHM)

Dawid Budnicki, Itxaso Parola, Krzysztof Markiewicz, Zbigniew Hołdyński, and Tomasz Nasiłowski are with the InPhoTech Sp. z o.o., 05-850 Ołtarzew, Poland (e-mail: dbudnicki@inphotech.pl; iparola@inphotech.pl; kmarkiewicz@inphotech.pl; zbigniew.holdynski@gmail.com; tnasilowski@inphotech.pl).

Łukasz Szostkiewicz is with the Polish Centre for Photonics and Fibre Optics, 20-061 Lublin, Poland (e-mail: lukasz.szostkiewicz@gmail.com).

Grzegorz Wojcik, Krzysztof Poturaj, and Paweł Mergo are with the Department of Optical Fiber Technology, Marie Curie-Sklodowska University, 20-031 Lublin, Poland (e-mail: grzegorzwojcik@poczta.umcs.lublin.pl; potkris@poczta.umcs.lublin.pl; pawel.mergo@poczta.umcs.lublin.pl).

Mariusz Makara is with the Department of Optical Fiber Technology, Marie Curie-Sklodowska University, 20-031 Lublin, Poland, and also with the Polish Centre for Photonics and Fibre Optics, 20-061 Lublin, Poland (e-mail: m.makara@poczta.umcs.lublin.pl).

Małgorzata Kuklińska and Marek Napierała are with the Polish Centre for Photonics and Fibre Optics, 20-061 Lublin, Poland (e-mail: mkuklinska@pcfs.org.pl; mnapierala@pcfs.org.pl).

Color versions of one or more of the figures in this article are available online at https://ieeexplore.ieee.org.

Digital Object Identifier 10.1109/JLT.2020.3012769

and mechanical engineering. Due to the numerous advantages of fiber optic sensors in comparison to electrical ones (e.g. small size, lightweight, electromagnetic interference immunity, corrosion-resistance and high sensitivity), optical fiber sensors are developed as a powerful and rich technology for bend-sensing in a variety of applications. For instance, they are used for real-time monitoring of the state and the safe operation of multiple infrastructures such as bridges, roads or pipelines [1]–[3]. Optical fiber bend sensors have also found a niche market in physiotherapy and medicine as they can detect human posture or track the orientation of robotic arms [4], [5]. Since optical sensors are lightweight and easy to embed in a variety of materials, the manufacturing of robotic arms can be carried out in lighter materials such as composites. This solution will allow their movements to be sped up, thus increasing their productivity.

The fiber-optic bend sensors developed so far are mainly based on interferometric methods [6]–[11], fiber Bragg gratings (FBGs) [12]–[14], or long period fiber gratings (LPGs) [15], [16]. Some of the interferometric bend sensors reported thus far present high sensitivity [6], but their manufacturing is complex. On the other hand, the fabrication of FBG and LPG based sensors also presents many difficulties and their sensitivity to the environmental conditions that surrounds the sensor can introduce uncertainty into the measurement and negatively influence the bending interpretation, resulting in a requirement for additional sensors as reference in some cases. The unique features of multicore fibers (MCFs) open new possibilities for the fabrication of bend sensors using a variety of methodologies. Detecting both the bending orientation and angle is crucial in reliably estimating the shape of the fiber and thereby, the shape of the element being sensed. Recently, distributed sensing techniques have been explored for the detection of bending using MCF like Brillouin optical time domain analysis (BOTDA) [17], and more recently phase-sensitive optical time-domain reflectometry (ϕ-OTDR) [18], which presents a higher sensitivity level. These techniques allow both bending orientation and radius to be detected, but distributed sensing requires complex architectures and interrogations systems, which increases the difficulty and costs of such systems. In [19], an interferometric bend sensor based on a strongly coupled three-core MCF was reported in which combining the intensity interrogation and the spectral interrogation of the interference pattern, it can distinguish multiple bending orientations. Another sensor capable of distinguishing bending orientation and curvature simultaneously was proposed

in [20] based on an asymmetrically structured three-core-fiber. This sensor reported recognition of multiple directions and small cross sensitivity with temperature. Both [19] and [20] present vector sensors that are promising and simple to fabricate, but they require a spectrum analyzer to extract the spectral data, which increases the cost and size.

In this paper we present, to the best of our knowledge, the first optical fiber bend sensing solution based on differential light-intensity variations in a micro-structured 7-core MCF with an asymmetric air-hole structure. Due to this asymmetric structure of air-holes, each of the 6 sensing cores of the MCF is characterized by presenting different confinement losses of the fundamental mode at different bends. This feature allows the detection of the bending intensity and orientation in the full 360° range with no dead-zones and a precision in the fiber-end detection of millimeter resolution by just employing a power meter as a detector. Moreover, the unique hole-assisted structure of the MCF guarantees low cross talk between the cores. The presented method of intensity-measurement provides for simplicity of the architecture and robustness in comparison to other conventional techniques for vector bending sensing.

II. PRINCIPLE OF OPERATION AND EXPERIMENTAL SETUP

The all-fiber bend sensor proposed in this paper is based on the fact that the confinement losses in MCFs depend on the geometry of the air-hole structure that surrounds the core [21]. Therefore, when designing a micro-structured fiber with an asymmetrical structure of air holes, it is possible to obtain an increased bending-sensitivity in a specific direction, while eliminating it in the opposite direction. Our design of such a bend-sensitive structure is shown in Fig. 1(a). As can be seen, the micro-structured cell presented has air-holes of a constant size and a constant lattice parameter, but the arrangement of the air-holes is asymmetrical. This causes changes in the confinement loss of the fundamental mode when the optical fiber is bent and leads to shifts in the mode field distribution [22]. Fig. 1(b) (c) and (d) illustrate the mode field distribution of the presented bend-sensitive cell for three different bending situations simulated employing the methodology described in [22] for a tip deviation of 4.65 cm: (b) no bending (straight fiber); (c) bending toward a single ring of air-holes; and (d) bending in the direction of three rings of air-holes. When the mode is shifted towards a single ring of air holes it experiences higher confinement loss, as the single hole ring is not capable of surpassing the evanescent field, and thus the mode leaks faster. On the other hand when the mode is shifted towards a triple line of holes, the mode exhibits lower confinement loss, as the vast air hole structure efficiently creates a low loss waveguide [23].

The orientation-sensitivity of the proposed fiber sensor depends on the number of bend-sensitive cells. A single-cell structure can detect changes in a specific range of angles, and thus, using a multiple-cell design it is possible to sense bending radius and orientation in a full range of angles (0° - 360°). In our approach, we fabricated a fiber consisting of six bend-sensitive cells spaced 60° apart from each other, which provides adequate sensitivity in the full range of angles (see
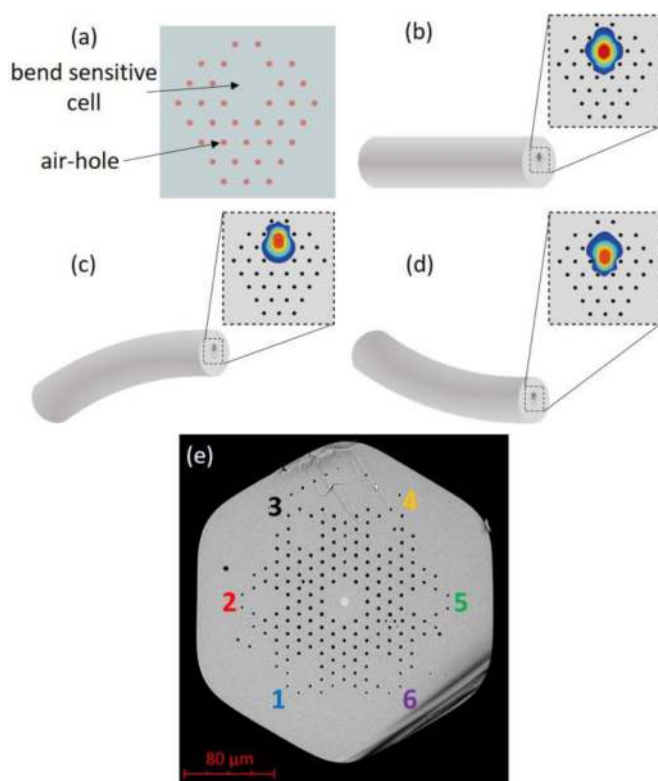

Fig. 1. Visualization of the bend-sensitive microstructured cell (a) and the mode field distribution for different fiber bends: unbent fiber (b); a fiber bent towards a region of a small number of air-holes (c); and a fiber bent towards an area with a big number of air-holes (d). Cross-section of the manufactured MCF based on six bend-sensitive cells and a germanium-doped central-core (e).

the MCF cross section in Fig. 1(e)). This MCF was fabricated from silica using the stack and draw technique. The air-hole diameter is 3,5 μm and the lattice constant is fixed to 11,7 μm. Additionally, it presents a central-core doped with germanium (lighter color in Fig. 1(e)) developed in compliance with the ITU-T G.652 recommendation for providing single-mode light propagation. This central core allows the stability of the system to be controlled by monitoring, for example, fluctuations in the power of the light source. Furthermore, the appropriate design of the air-hole structure in the MCF ensures practically no crosstalk between the cores, which guarantees the independent propagation of the signal through each core [24]. Fig. 2 illustrates the experimental setup employed throughout the measurements. A super-luminescent diode with a central wavelength of 1550 nm was used as the light source. The bend-sensing fiber has a length L of 15 cm, and it is attached to self-manufactured fan-in/fan-out elements at both ends, which converts the 7-core MCF into 7 ends with single-mode-fibers for allowing independent coupling and detection of light in each core of the MCF. The detection was carried out for each core using a photodiode power meter. The orientation and bending of the fiber were changed in a controlled manner by means of two rotation stages (0° - 360°) in the first case, and a point lateral displacement in the latter case. The first step in the experimental procedure was to measure the output power of each cell for a straight-fiber (no bending)
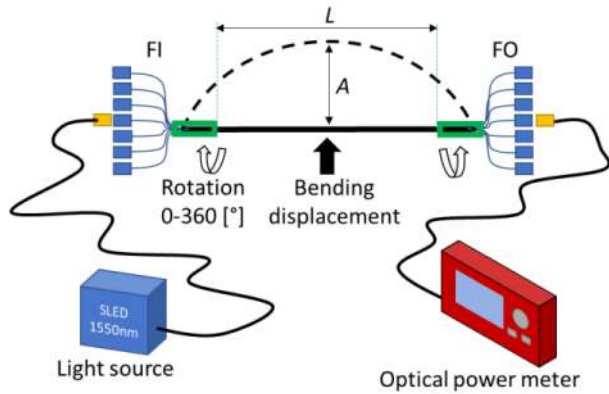
Fig. 2. Schematic of the measurement setup of the bending sensor. FI: fan-in; FO: fan-out; L: length of the bend-sensitive fiber; A: distance between the straight position and the maximum bent position.
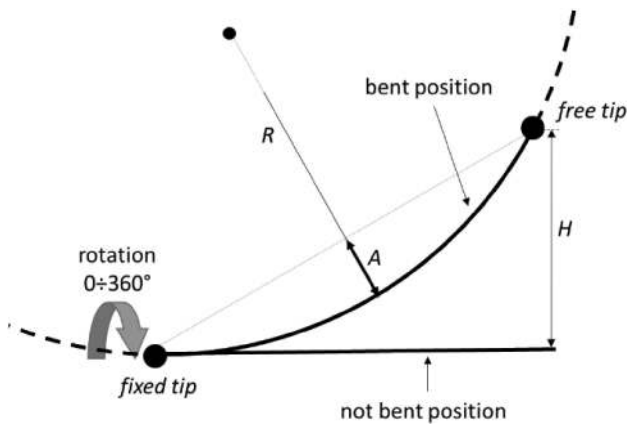

Fig. 3. Schematic representation of the relationship between R, A and H for a specific bending simulating real conditions with a fixed tip and a free tip.

position and 0° of rotation. Then, the bending displacement was increased stepwise and the power measurements of each core were repeated in each step. Once the maximum bending was reached, the orientation of the fiber was changed in steps of 15° and the procedure was repeated. Every single bend angle and orientation configuration provides different loss values in each core, and on the basis of these values, it is possible to determine the direction and the level of bending.

The bending radius of the sensing fiber can be determined according to the following dependence:

$$R = \frac{A^2 + \left(\frac{L}{2}\right)^2}{2A} \qquad (1)$$

where L is the length of the sensing fiber, and A represents the distance between the straight and the maximum bent positions of the fiber. This relationship is schematically illustrated in Fig. 3. In order to make the analysis and representation of the bending level easier, we converted the bending radius into the so-called tip deviation (H). It simulates the situation where one of the fiber ends is immobilized and the other end is free and susceptible to position changes due to the applied bending. Therefore, H represents the position change of the free fiber tip from the
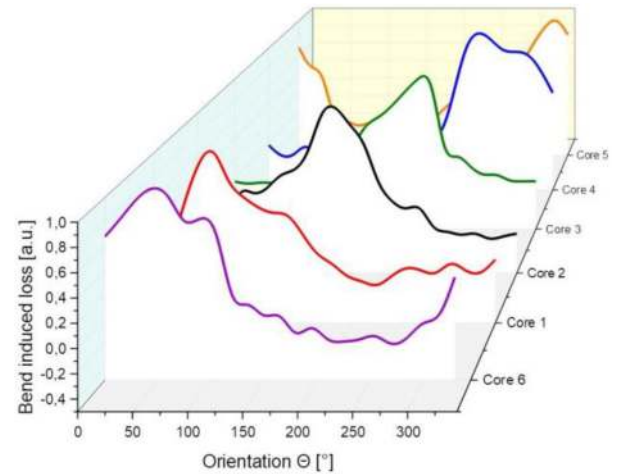

Fig. 4. Relationship between optical losses and probe rotation of each bend-sensitive core of the tested sensor for a tip deviation of H = 1,2 cm from the straight position.

original straight position to the new location after bending (see Fig. 3). The value of H can be determined from the following relation:

$$H = \sqrt{\left(L - R\sin\left(\frac{L}{R}\right)\right)^2 + \left(R - R\cos\left(\frac{L}{R}\right)\right)^2} \qquad (2)$$

III. RESULTS

A. Experimental Results

Each bend-sensitive cell is responsive to a range of fiber orientation angles, presenting a maximum loss value at a specific angle. For the purpose of characterizing the response of each core, the probe was tested for the full range of fiber orientation ($\Theta = 0° - 360°$) in steps of 15° and up to a maximum bending level corresponding to a tip deviation H = 1,4 cm. Fig. 4 illustrates the measured optical losses of each sensitive core for a tip deviation H = 1,2 cm. The loss curves have been normalized to 1 with respect to the maximum loss value of each core for the clarity of the plot. As can be seen, each core shows significant losses for a specific range of bending angles, covering at least a range of 80°. In addition, the response of each core is partially superimposed with the response of the adjacent cores, and therefore our MCF sensor does not have dead-zones and ensures its reliability in 360° of rotation.

Apart from monitoring the bending orientation, our sensor is also capable of detecting the value of the tip deviation (H). On the one hand, Fig. 5 shows the evolution of the optical losses of one of the sensitive cores as a function of the fiber orientation for four different tip deviations. As can be observed, a greater tip deviation (greater bending) causes greater losses in the propagated light. This result could be expected as a greater bending in an optical fiber increases the confinement losses [23]. It should be noted that the signal amplification (negative losses) represented in this graph is caused due to the fact that the transmitted light has lower propagation losses when the mode is
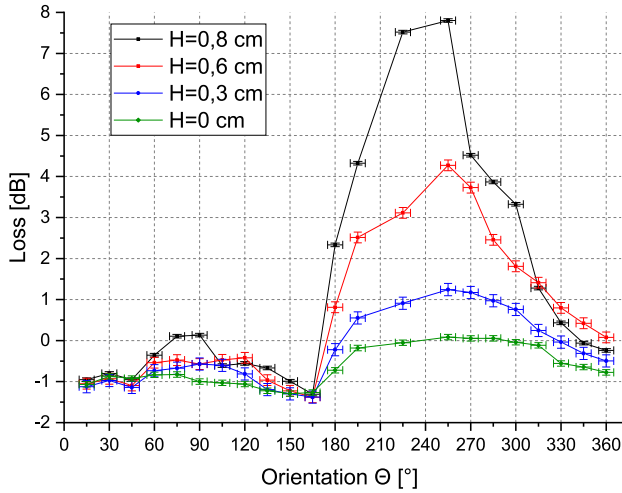
Fig. 5.   Evolution of the optical losses of one of the bend-sensitive cores as a function of the bending orientation and 4 different tip deviations (H).
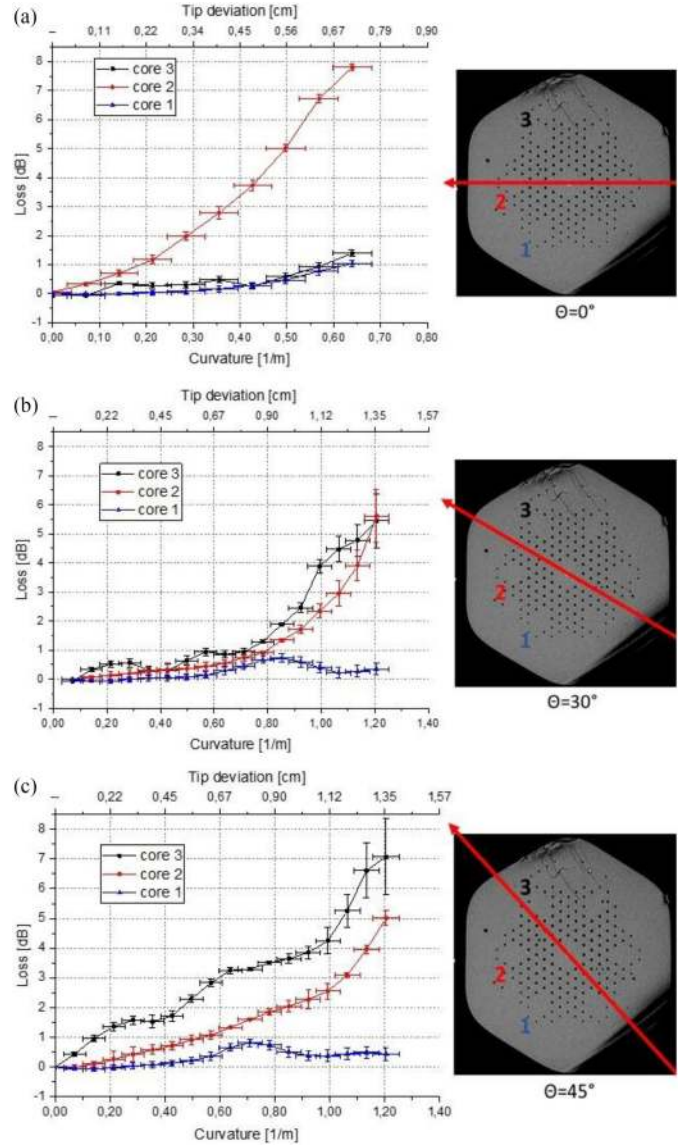

Fig. 6.   Relationship between optical losses with curvature and tip deviation for three neighboring cores and three different bending orientations: (a) $\Theta = 0°$ (bending toward core 2); (b) $\Theta = 30°$ (bending between cores 2 and 3); and (c) $\Theta = 45°$ (asymmetric bending closer to core 3 than to core 2). Only 3 of the 6 cores are presented for the sake of clarity.

shifted toward the triple line of holes than when it is propagated through a straight fiber (which is the reference measurement to calculate the losses).

On the other hand, Fig. 6 shows the characterization of the optical losses as function of the tip deviation. The analysis was carried out for three neighboring cores and three different bending orientations with the purpose of demonstrating the selective response of each core to rotation. The standard deviation of the measured optical losses is ± 0.05 dB calculated based on three complete rounds of measurements for each core. Fig. 6(a) corresponds to a bending orientation towards the axis of core 2 ($\Theta = 0°$), which causes significant losses in this core increasing quite abruptly with the tip deviation. Due to the symmetric structure of our MCF, the applied bending causes the modes of cores 1 and 3 to shift toward the same number of air-holes. Therefore, these two cores present practically the same losses with a smooth increase with the tip deviation. Similarly, in Fig. 6(b) we bent the fiber 30° (between cores 2 and 3), and as expected, this caused comparable losses in cores 2 and 3 presenting a moderate slope with the tip deviation. As can be seen, the response of core 1 to this bending orientation is practically negligible. Lastly, Fig. 6(c) represents the case of an asymmetric response of cores 2 and 3 ($\Theta = 45°$). As can be seen, the bend-sensitivity of core 3 is greater than that of core 2, as their modes are shifted asymmetrically in each cell. In this case again the sensitivity of core 1 is negligible. From these results it is demonstrated that our MCF sensor can detect bending changes with a resolution of few millimeters based on specific optical loss measurements. It should be mentioned that the range of detectable tip deviation could be further increased by using a light source with a higher optical power.

It should be noted that all the experimental measurements were carried out for a sensor length of 15 cm. However, the sensitivity in measuring the curvature depends on the optical fiber length. This dependency is illustrated in Fig. 7., for the sake of clarity. As can be seen, different curvatures (or bending radii) applied to the fiber correspond to different loss as the sensor

length varies. Therefore, the sensitivity of the presented bend-sensor shows a dependency with the fiber length as presented in Fig. 7.

B. Theoretical Reconstruction of the Bending Angle and Tip Deviation

In order to theoretically reconstruct the bend angle and tip deviation based on the loss measurements of the proposed fiber, we have followed a method similar to the one presented in [18]. From the measurement data we created 6 points in a 3D space defined as:

$$P_i = \begin{bmatrix} x_i \\ y_i \\ z_i \end{bmatrix} \qquad (3)$$
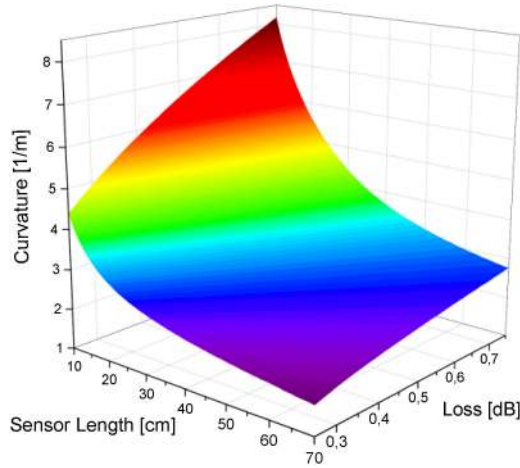
Fig. 7.   Illustration of the response of the sensitivity of the sensor as function of the optical fiber length.

where x_i, and y_i represent the location of i-th core in the cross-section of the fiber, and z_i depicts the losses in dBs of the i-th core. In the next step, a plane was fitted to the defined points using the least square method. The normal vector to the calculated plane is defined as (where the sub-index depicts calculated):

$$N = \begin{bmatrix} x_c \\ y_c \\ z_c \end{bmatrix} \qquad (4)$$

Based on the normal vector parameters, the bending angle and tip deviations were calculated using the following equations:

$$\Theta = \begin{cases} \tan^{-1}\left(\frac{y_c}{x_c}\right) & x_c \geq 0 \\ \tan^{-1}\left(\frac{y_c}{x_c}\right) + \pi & x_c < 0 \end{cases} \qquad (5)$$

$$H = \frac{z_c}{|N|} \qquad (6)$$

Based on the previous equations, and by using the experimental loss measurements as a starting point, the theoretical reconstruction of the bending angle and tip deviation has been carried out. Fig. 8 shows a comparison of the experimentally applied and theoretically reconstructed bending orientation and tip deviation, each for three cases. As can be seen, the theoretically reconstructed values match accurately the experimentally applied values in all cases for both graphs. It should be noted that the bumps shown in Fig. 8(a) around an orientation of 130° and in Fig. 8(b) around a tip deviation of 1 cm may be due to matching the conditions for interference between the cladding mode and the mode propagating through the core, which provides inaccurate measurement data, and therefore a mismatch between the experimental and theoretical values.

Finally, the reliability of the proposed sensor is calculated from the standard deviation of the differences between pairs of measured data and reconstructed data. We determined the sensor accuracy as 20° in bending angle and 1.5 mm in tip deviation, for measurements of bending angles ranging from 0° to 345° with steps of 15° and tip deviations ranging from 0 to 1.6 cm with steps of 0.8 mm.
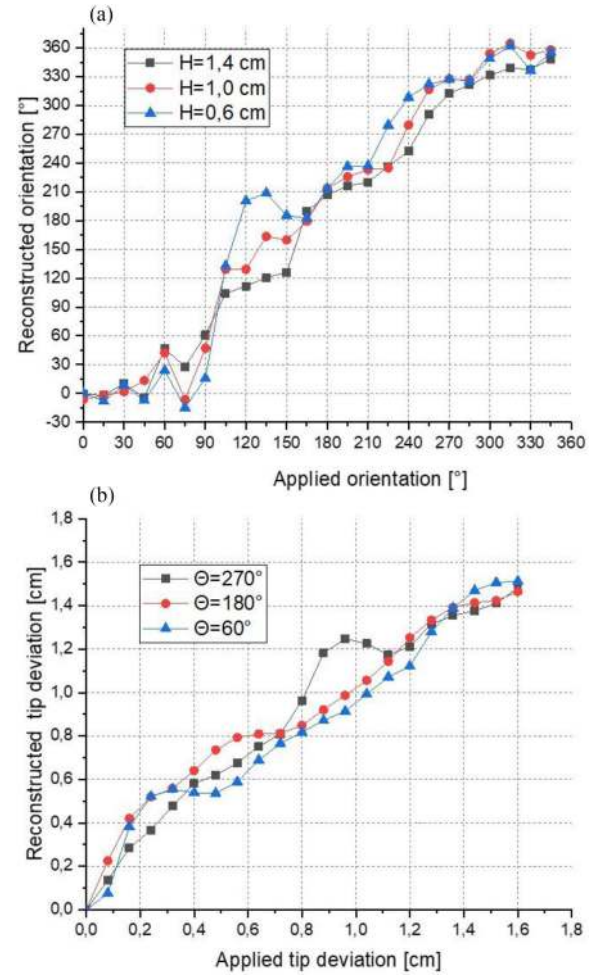

Fig. 8.   Comparison between (a) applied and reconstructed bending angle for a tip deviation of 0.6, 1 and 1.4 cm, and (b) applied and reconstructed tip deviation for a bending angle of 60°, 180° and 300°.

IV. CONCLUSION

We reported the implementation of a self-fabricated micro-structured 7-core multicore fiber as a vector bend sensor based on intensity measurement. Six cores serve as bend-sensitive cells, while the central core allows the stability of the sensor system to be measured. The experimental results confirm the sensor's ability to detect bends in a range of 0° - 360° without any dead-zones, and millimetric accuracy on the fiber-tip detection of 1.5 mm. The presented method, unlike other conventional solutions, presents low cross-sensitivity to external factors, simplicity of the architecture and robustness of the system. We believe the reported MCF-based sensor presents potential features to pave the way for cheap and efficient vector bending sensors.

REFERENCES

[1] C. K. Y. Leung *et al.*, "Review: Optical fiber sensors for civil engineering applications," *Mater. Struct.*, vol. 48, no. 4, pp. 871–906, 2013, doi: 10.1617/s11527-013-0201-7.

[2] G. Rajan, B. G. Prusty, and K. Iniewski, *Structural health monitoring of composite structures using fiber optic methods*. Boca Raton, Florida: CRC Press Taylor & Francis Group, 2017.

[3] X. W. Ye, Y. H. Su, and J. P. Han, "Structural health monitoring of civil infrastructure using optical fiber sensing technology: A comprehensive review," *Sci. World J.*, vol. 2014, pp. 1–11, 2014, doi: 10.1155/2014/652329.

[4] S. Sareh, Y. Noh, M. Li, T. Ranzani, H. Liu, and K. Althoefer, "Macrobend optical sensing for pose measurement in soft robot arms," *Smart Mater. Struct.*, vol. 24, no. 12, 2015, Art. no. 125024, doi: 10.1088/0964-1726/24/12/125024.

[5] A. Schmitz, A. J. Thompson, P. Berthet-Rayne, C. A. Seneci, P. Wisanuvej, and G. Z. Yang, "Shape sensing of miniature snake-like robots using optical fibers," in *Proc. IEEE Int. Conf. Intell. Robot. Syst.*, 2017, pp. 947–952, doi: 10.1109/IROS.2017.8202259.

[6] Q. Wang and Y. Liu, "Review of optical fiber bending/curvature sensor," *Meas. J. Int. Meas. Con.*, vol. 130, pp. 161–176, 2018, doi: 10.1016/j.measurement.2018.07.068.

[7] Y. Gong, T. Zhao, Y. J. Rao, and Y. Wu, "All-fiber curvature sensor based on multimode interference," *IEEE Photon. Technol. Lett.*, vol. 23, no. 11, pp. 679–681, Jun. 2011.

[8] H. P. Gong, C. C. Chan, P. Zu, L. H. Chen, and X. Y. Dong, "Curvature measurement by using low-birefringence photonic crystal fiber based Sagnac loop," *Opt. Commun.*, vol. 283, no. 16, pp. 3142–3144, 2010, doi: 10.1016/j.optcom.2010.04.023.

[9] M. J. Gander *et al.*, "Two-axis bend measurement using multicore optical fibre," *Opt. Commun.*, vol. 182, no. 1–3, pp. 115–121, 2000, doi: 10.1016/S0030-4018(00)00817-8.

[10] Y. Wu *et al.*, "Highly sensitive curvature sensor based on asymmetrical twin core fiber and multimode fiber," *Opt. Laser Technol.*, vol. 92, no. January, pp. 74–79, 2017, doi: 10.1016/j.optlastec.2017.01.007.

[11] C. Li *et al.*, "All-fiber multipath Mach–Zehnder interferometer based on a four-core fiber for sensing applications," *Sens. Actuators, A Phys.*, vol. 248, pp. 148–154, 2016, doi: 10.1016/j.sna.2016.07.031.

[12] L. Y. Shao, A. Laronche, M. Smietana, P. Mikulic, W. J. Bock, and J. Albert, "Highly sensitive bend sensor with hybrid long-period and tilted fiber Bragg grating," *Opt. Commun.*, vol. 283, no. 13, pp. 2690–2694, 2010, doi: 10.1016/j.optcom.2010.03.013.

[13] W. Bao, Q. Rong, F. Chen, and X. Qiao, "All-fiber 3D vector displacement (bending) sensor based on an eccentric FBG," *Opt. Express*, vol. 26, no. 7, 2018, Art. no. 8619, doi: 10.1364/oe.26.008619.

[14] W. Cui, J. Si, T. Chen, and X. Hou, "Compact bending sensor based on a fiber Bragg grating in an abrupt biconical taper," *Opt. Express*, vol. 23, no. 9, 2015, Art. no. 11031, doi: 10.1364/oe.23.011031.

[15] D. Zhao *et al.*, "Implementation of vectorial bend sensors using long-period gratings UV-inscribed in special shape fibres," *Meas. Sci. Technol.*, vol. 15, no. 8, pp. 1647–1650, 2004, doi: 10.1088/0957-0233/15/8/037.

[16] P. Geng *et al.*, "Two-dimensional bending vector sensing based on spatial cascaded orthogonal long period fiber," *Opt. Express*, vol. 20, no. 27, 2012, Art. no. 28557, doi: 10.1364/oe.20.028557.

[17] Z. Zhao, M. A. Soto, M. Tang, and L. Thévenaz, "Distributed shape sensing using Brillouin scattering in multi-core fibers," *Opt. Express*, vol. 24, no. 22, 2016, Art. no. 25211, doi: 10.1364/OE.24.025211.

[18] Ł. Szostkiewicz *et al.*, "High-resolution distributed shape sensing using phase-sensitive optical time-domain reflectometry and multicore fibers," *Opt. Express*, vol. 27, no. 15, 2019, Art. no. 20763, doi: 10.1364/oe.27.020763.

[19] J. Villatoro, A. Van Newkirk, E. Antonio-Lopez, J. Zubia, A. Schülzgen, and R. Amezcua-Correa, "Ultrasensitive vector bending sensor based on multicore optical fiber," *Opt. Lett.*, vol. 41, no. 4, p. 832, 2016, doi: 10.1364/ol.41.000832.

[20] S. Wang *et al.*, "Two-dimensional bending vector sensor based on the multimode-3-core-multimode fiber structure," *IEEE Photon. Technol. Lett.*, vol. 29, no. 10, pp. 822–825, May 2017, doi: 10.1109/LPT.2017.2687480.

[21] T. P. White, R. C. McPhedran, C. M. de Sterke, L. C. Botten, and M. J. Steel, "Confinement losses in microstructured optical fibers," *Opt. Lett.*, vol. 26, no. 21, 2001, Art. no. 1660, doi: 10.1364/ol.26.001660.

[22] R. T. Schermer and J. H. Cole, "Improved bend loss formula verified for optical fiber by simulation and experiment," *IEEE J. Quantum Electron.*, vol. 43, no. 10, pp. 899–909, Oct. 2007, doi: 10.1109/JQE.2007.903364.

[23] T. Wu, L. Dong, and H. Winful, "Bend performance of leakage channel fibers," *Opt. Express*, vol. 16, no. 6, 2008, Art. no. 4278, doi: 10.1364/oe.16.004278.

[24] L. Szostkiewicz, M. Napierala, A. Ziolowicz, A. Pytel, T. Tenderenda, and T. Nasilowski, "Cross talk analysis in multicore optical fibers by supermode theory," *Opt. Lett.*, vol. 41, no. 16, 2016, Art. no. 3759, doi: 10.1364/ol.41.003759.